

PHASE-FIELD MODELING OF DENDRITIC SOLIDIFICATION IN UNDERCOOLED DROPLETS

P.K. GALENKO, D.M. HERLACH, G. PHANI KUMAR, O. FUNKE

Institute of Space Simulation, DLR, 51170, Cologne, Germany

The predictions of a phase-field model for dendritic growth with forced convective flow of the liquid phase are tested in comparison with experimental data on solidification of nickel droplets in electromagnetic levitation facility. It is shown that small amounts of impurities and forced convective flow can lead to an enhancement of the velocity of dendritic solidification at small undercoolings.

1. INTRODUCTION

Different techniques have been applied for measurement of dendritic growth velocities during solidification of electromagnetically levitated melts, e.g. the usage of a fast responding photo-double-diode¹ or an ultra-high-speed camera system². The LKT model of dendrite growth³ predicts the dendrite growth velocity V as a function of the undercooling ΔT in good agreement with experimental data for nickel solidification only in the region of medium undercoolings $100 \text{ K} < \Delta T < 200 \text{ K}$ (see Ref.¹). Recently, we suggested a modification to the LKT model which takes into account the effect of forced convective flow caused by electromagnetic stirring⁴. The modified model predicts the increase of velocity when the flow is directed opposite to the dendrite growth. However, the effect of forced convective flow alone can still not explain the measured data satisfactorily⁴. The additional reason for dendrite velocities higher than predicted by the model might be due to the presence of small amounts of impurities which may drastically influence the kinetics of solidification⁵. Therefore we present the phase-field model predictions in comparison with the measurements of dendrite velocity. To test the influence of a small amount of impurity, the functions $V-\Delta T$ are presented for the Ni dendrites in comparison with a very dilute alloy of Ni.

2. GOVERNING EQUATIONS

We have used the phase-field model via "thin-interface" analysis⁶ where the interface thickness W_0 is assumed to be small compared to the scale of the crystal but not smaller than the microscopic capillary length d_0 . The phase-field and energy equations were taken from Ref.⁷ with the momentum and continuity equations for the liquid taken from Ref.⁸. Furthermore, in the momentum equation, the Lorentz force caused by the alternating electromagnetic field, has been introduced for an undercooled levitated droplet. A system of governing equations is described by

- *energy conservation*

$$\frac{\partial T}{\partial t} + (1 - \varphi)(\vec{v} \cdot \nabla)T = a\nabla^2 T + \frac{T_Q}{2} \frac{\partial \Phi}{\partial t}, \quad (1)$$

- *continuity of the liquid phase*

$$\nabla \cdot [(1 - \varphi)\vec{v}] = 0, \quad (2)$$

- *momentum transfer*

$$(1 - \varphi)(\vec{v} \cdot \nabla)\vec{v} = -\frac{1 - \varphi}{\rho}\nabla p + \frac{(1 - \varphi)}{\rho}\vec{F}_{LZ} + \nabla \cdot \left[\frac{\mu}{\rho}\nabla(1 - \varphi)\vec{v} \right] + \vec{F}_D, \quad (3)$$

- *phase-field evolution*

$$\tau(\vec{n})\frac{\partial \Phi}{\partial t} = \nabla \cdot (W^2(\vec{n})\nabla \Phi) + \sum_{w=x,y,z} \frac{\partial}{\partial w} \left(|\nabla \Phi|^2 W(\vec{n}) \frac{\partial W(\vec{n})}{\partial (\partial_w \Phi)} \right) - \frac{\partial F}{\partial \Phi}. \quad (4)$$

In Eqs. (1)-(4), T is the temperature, T_Q is the adiabatic temperature of solidification defined by $T_Q = Q/c_p$, Q is the latent heat of solidification, c_p is the specific heat, a is the thermal diffusivity, Φ is the phase-field variable ($\Phi=1$ is the liquid phase and $\Phi=0$ is for the solid phase); $\varphi=(1+\Phi)/2$ is the fraction of the solid phase ($\varphi=0$ is for the liquid and $\varphi=1$ is for the solid), \vec{v} is the fluid flow velocity in the liquid, x,y,z are the Cartesian coordinates, t is the time, ρ is the density, μ is the dynamic viscosity, and p is the pressure. The dissipative force F_D in the Navier-Stokes equation (3) is taken from Ref.⁸. Furthermore, in solution of Eq. (3), the Lorentz force has been averaged in time: $F_{LZ} \approx |B|^2/(4\pi\delta)$, where $|B| = B_0 \exp[(r-R_0)/\delta]$ is the modulus of the magnetic induction vector, B_0 is the time averaged value of the magnetic induction, r is the radial distance of a droplet of radius R_0 , $\delta = [2/(\omega\sigma_R\mu_0)]^{1/2}$ is considered as a skin depth for the alternating magnetic field in the droplet, which decreases for a

short distance at which the modulus of magnetic induction $|B|$ decays exponentially (where ω is a frequency of the applied current, σ_R is the electric conductivity, and μ_0 is the magnetic permeability). The phenomenological free energy F is defined by $F(T, \Phi) = f(\Phi) + \lambda(T - T_M)g(\Phi)/T_Q$, where T_M is the equilibrium temperature of solidification. With including the double-well function $f(\Phi) = -\Phi^2/2 + \Phi^4/4$ and the odd function $g(\Phi) = \Phi - 2\Phi^3/3 + \Phi^5/5$ itself, the free energy F is constructed in such a way that a tilt λ of an energetic well controls the coupling for T and Φ .

The time $\tau(\vec{n})$ of the phase-field kinetics and the thickness $W(\vec{n})$ of the anisotropic interface are given by

$$\tau(\vec{n}) = \tau_0 a_c(\vec{n}) a_k(\vec{n}) \left[1 + a_2 \frac{\lambda d_0}{a \beta_0} \frac{a_c(\vec{n})}{a_k(\vec{n})} \right], \quad W(\vec{n}) = W_0 a_c(\vec{n}), \quad (5)$$

where τ_0 is the time-scale for the phase-field kinetics, W_0 is the parameter of the interface thickness with $W_0 = \lambda d_0 / a_1$, and $a_1 = (5/8)^{1/2}$. The second term in brackets of Eq. (5) for $\tau(\vec{n})$ defines a correction $a_2 = 0.6267$ for the "thin-interface" asymptotic¹².

The anisotropy of interfacial energy is given by

$$a_c(\vec{n}) = \frac{\gamma(\vec{n})}{\gamma_0} = (1 - 3\varepsilon_c) \left[1 + \frac{4\varepsilon_c}{1 - 3\varepsilon_c} (n_x^4 + n_y^4 + n_z^4) \right], \quad (6)$$

where $\gamma(\vec{n})$ is the surface energy dependent on the normal vector \vec{n} to the interface, γ_0 is the mean value of the interfacial energy along the interface, and ε_c is the anisotropy parameter. The anisotropy of kinetics of atomic attachment to the interface is given by

$$a_k(\vec{n}) = \frac{\beta(\vec{n})}{\beta_0} = (1 + 3\varepsilon_k) \left[1 - \frac{4\varepsilon_k}{1 + 3\varepsilon_k} (n_x^4 + n_y^4 + n_z^4) \right], \quad (7)$$

where $\beta(\vec{n})$ is the kinetic coefficient dependent on the normal vector \vec{n} to the interface, β_0 is the averaged kinetic coefficient along the interface which is defined by $\beta_0 = (\mu_{100} - \mu_{110})/(2T_Q)$, and $\varepsilon_k = (\mu_{100} - \mu_{110})/(1/\mu_{100} + 1/\mu_{110})$ is the kinetic anisotropy parameter in which μ_{100} and μ_{110} are the kinetic coefficients in the <100>- and <110>-direction, respectively. In Eqs. (5)-(7), the normal vector has the components (n_x, n_y, n_z) defined by the gradients of the phase-field as follows

$$n_x^4 + n_y^4 + n_z^4 = [(\partial\Phi/\partial x)^4 + (\partial\Phi/\partial y)^4 + (\partial\Phi/\partial z)^4]/|\Phi|^4.$$

3. RESULTS AND DISCUSSION

Equations (1)-(7) have been solved numerically by a finite-difference technique on a uniform computational grid. We used a multi-grid algorithm for resolving the equations of the phase-field (4), heat transfer (1) and momentum (3) which have the different spatial lengths and time scales of their dynamics. Parameters of modeling and material parameters for pure nickel are given in Ref.⁵

3.1. Dendritic patterns

We obtained the morphological spectrum of interfacial crystal structures for a wide range of undercoolings. In our modeling, the spectrum of the crystal structures obtained exhibits a change from grained crystals at very small undercoolings ($\Delta T < 0.15T_Q$) to dendritic patterns at intermediate undercoolings ($0.1T_Q < \Delta T < 1.0T_Q$) to grained crystals again at high undercoolings ($\Delta T > 1.0T_Q$). Within the range of intermediate undercoolings, the shape of dendrites is dictated by the preferable crystallographic direction (which is $<100>$ -direction for the case of Ni). Furthermore, stochastic noise plays a crucial role in the formation of branched crystal patterns of dendritic type. Figure 1(a) shows the dendritic crystal with secondary branches with the application of the thermal noise. Solidification under the influence of forced convective flow in a droplet produces dendritic growth pronounced in the direction opposite to that of the far field flow velocity U_0 (see Ref.⁴). The present results of modeling also confirm this outcome: with the imposing of the fluid flow, the growth becomes pronounced in the direction opposite to the flow as shown in Fig. 1(b). For these structures, i.e. with the thermal noise in a stagnant melt and also with the melt flow (Fig. 1) we compared the results for dendrite growth velocity V in pure Ni versus undercooling ΔT quantitatively.

The results of phase-field modeling exhibit an increase of the velocity of the upstream dendritic branch, Fig.2. As soon as the thermal boundary layer shrinks ahead of the up-stream branch due to the flow, the heat of solidification is removed better, and the growth velocity enhances. The enhanced dendrite velocity due to the melt flow decreases the discrepancy between theory and experimental data at small undercoolings. Hence we have compared the predictions of the present phase-field modeling with the new experimental data⁵ for growth kinetics of nickel dendrites.

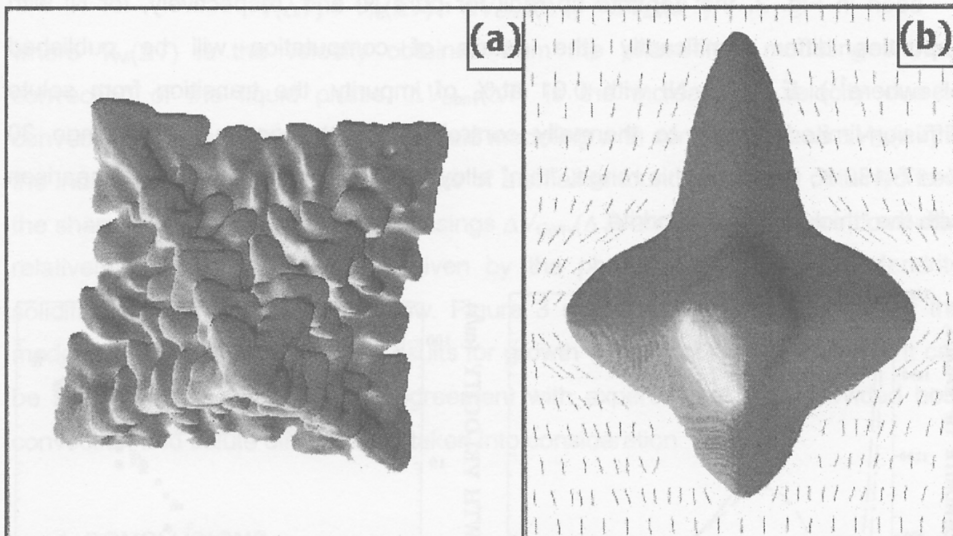


Figure 1. (a) Dendritic growth pattern with side-branches due to application of finite level of thermal stochastic noise according to Reference⁹ with application to pure nickel at the undercooling $\Delta T = 0.55 T_Q$ (K). Pattern has been simulated on a grid of size 650^3 nodes. (b) Growth of nickel dendrite under convective flow at $\Delta T = 0.30 T_Q$ (K) and $U_0 = 0.7$ (m/s). Growth velocity of the up-stream branch is pronounced in comparison with the down-stream branch due to forced convection. Dashed lines around the dendrite indicate the flow velocity vectors in the vertical cross-section. Pattern has been simulated on a grid of size $230 \times 230 \times 330$ nodes.

3.2. Comparison with experimental data

We improved the accuracy of the CPS technique and performed new measurements of dendritic velocities in levitated nickel samples⁵. The measurements were performed for dendritic growth velocity V as a function of undercooling $\Delta T = T_L - T_\infty$, measured experimentally for the melted drop. Here, T_L is the liquidus temperature, and T_∞ is the actual temperature of the drop. Solidification of the melt was triggered in the range of $30 \text{ K} < \Delta T < 260 \text{ K}$.

Comparison of these new data with the solution of Eqs.(1)–(7) confirms that convection alone cannot describe the experimental results satisfactorily. The additional reason for the discrepancy that still exists might be due to the presence of small amounts of impurity⁵. Therefore, we have used the sharp-interface model¹⁰ to evaluate the influence of the solute diffusion on dendrite growth kinetics. As it can be

seen in Fig. 2, the dendrite tip radii for pure Ni and, respectively, for Ni with impurities differ significantly (the details of computation will be published elsewhere¹¹). E.g., for Ni with 0.01 at.% of impurity, the transition from solute diffusion-limited growth to thermally controlled growth occurs in the range $30 \text{ K} < \Delta T < 130 \text{ K}$, Fig. 2. In this range, "thin" alloy dendrites grow rapidly in comparison with the "thick" thermal dendrite.

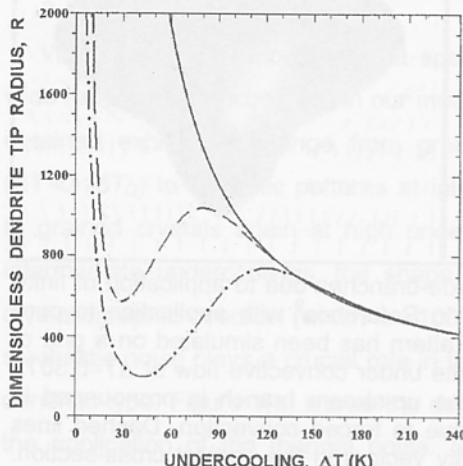


Figure 2. Dendrite tip radius as a function of undercooling. Solid line is for pure Ni, dashed line is for Ni 0.01 at. % of impurity, and dashed-dotted line is for Ni with 0.05 at.% of impurity.

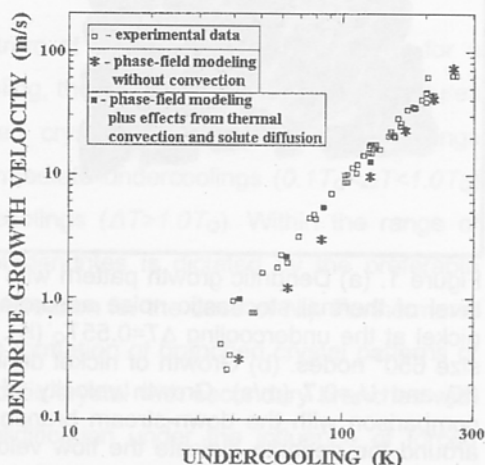


Figure 3. Comparison of data from experiment (open squares), phase-field modeling for pure Ni without flow (stars), and final data (black squares) with the effect from thermal convection and solute diffusion.

Consequently, we have found that small amounts of impurities in nickel can lead to an enhancement of the growth velocity but with a temperature characteristic being different from that of the effect by fluid flow. This allows to discriminate between both contributions and model them separately by means of the phase-field modeling of dendrite solidification with convective flow and the sharp-interface model of dendritic growth of a binary system. Therefore, using the results of the present phase-field modeling for pure nickel, Eqs. (1)-(7), and the sharp-interface model¹⁰ for Ni + 0.01 at.% of impurity, we determined the final growth velocity as follows:

$$V(\Delta T) = V_{Ni}(\Delta T) + \Delta V_{Conv}(\Delta T) + \Delta V_{Diff}(\Delta T),$$

where $V_{Ni}(\Delta T)$ is the velocity obtained from the phase-field modeling without convection of the liquid phase, $\Delta V_{Conv}(\Delta T)$ is the increase in velocity due to convection estimated from the phase-field modeling with convection, and $\Delta V_{Diff}(\Delta T)$ is the increase in velocity due to presence of a small amount of impurity obtained from the sharp interface model. The increasing $\Delta V_{Conv}(\Delta T)$ and $\Delta V_{Diff}(\Delta T)$ were computed relatively to the velocity $V_{Ni}(\Delta T)$ given by the phase-field modeling of dendrite solidification without convective flow. Figure 3 shows the final comparison of the modeling data and experimental results for growth velocity of nickel dendrites. It can be seen that we obtain a good agreement with experimental data provided both convection and solute diffusion are taken into consideration.

4. CONCLUSIONS

The results of phase-field model lead to the conclusion that forced convective flow enhances the growth velocity in the range of small undercoolings where the dendrite growth velocity is comparable to the velocity of the flow. Using the sharp interface model¹⁰, it is shown that even small amounts of impurity on the level of 0.01 at. % lead to an enhancement of the growth velocity in the range of small and intermediate undercoolings. The solute effect, however, shows a different temperature characteristics than the transport effect by fluid flow, which makes it possible to discriminate between both these effects by investigating the growth velocities as a function of undercooling.

ACKNOWLEDGEMENTS

The authors thank Prof. Wilfried Kurz and Prof. Christoph Beckermann for stimulating discussions and useful exchanges. Financial support of this work by Deutsche Forschungsgemeinschaft under the project No. HE 1601/13 is gratefully acknowledged.

REFERENCES

- 1) K. ECKLER, D.M. HERLACH, Mater. Sci. Eng. A **178** (1994) 159.
- 2) D.M. MATSON, The measurement of dendrite tip propagation velocity during growth into undercooled melts, in: Solidification 1998, eds. S.P. Marsh, J.A. Dantzig, R. Trivedi, W. Hofmeister, M.G. Chu, E.J. Lavrenia and J.-H. Chun, TMS, Warrendale PA, 1998.
- 3) J. LIPTON, W. KURZ, R. TRIVEDI, Acta Metall. **35** (1987) 957.
- 4) P.K. GALENKO, O. FUNKE, J. WANG, D.M. HERLACH, Mater. Sci. Eng. A (2004) in press.
- 5) O. FUNKE, G. PHANIUMAR, P.K. GALENKO, M. KOLBE, D.M. HERLACH, Phys. Rev. E (2004) submitted.
- 6) A. KARMA, W.-J. RAPPEL, Phys. Rev. E **57** (1998) 4323.
- 7) J. BRAGARD, A. KARMA, Y. H. LEE, M. PLAPP, Interface Science **10** (2002) 121.
- 8) C. BECKERMANN, H.-J. DIEPERS, I. STEINBACH, A. KARMA, X. TONG, J. Comp. Physics **154** (1999) 468.
- 9) A. KARMA, W.-J. RAPPEL, Phys. Rev. E **60** (1999) 3614.
- 10) P.K. GALENKO, D.A. DANILOV, Phys. Lett. A **235** (1997) 271.
- 11) P.K. GALENKO, D.M. HERLACH, G. PHANIUMAR, O. FUNKE, Phase-field modeling of solidification of undercooled melt: a test and comparison for the current models with the new experimental data. Manuscript in preparation, 2004.

ADVANCES IN SCIENCE AND TECHNOLOGY, 43

COMPUTATIONAL MODELING AND SIMULATION OF MATERIALS III

**Proceedings of the 3rd International Conference on
“Computational Modeling and Simulation of Materials”
Acireale, Sicily, Italy, May 30-June 4, 2004, Co-chaired by
Jean-Louis Barrat, Tomas Diaz de la Rubia and Masao Doi**

PART B

Edited by

P. VINCENZINI
World Academy of Ceramics

A. LAMI
National Research Council, Italy

TECHNA GROUP
Faenza 2004